Inorg. Chem. **2007**, *46*, 8710–8716

Accurate Computation of Reduction Potentials of 4Fe–4S Clusters Indicates a Carboxylate Shift in *Pyrococcus furiosus* Ferredoxin

Kasper P. Jensen,* Bee-Lean Ooi, and Hans E. M. Christensen

Department of Chemistry, Technical University of Denmark, Building 207, 2800 Kgs. Lyngby, Denmark

Received May 21, 2007

This work describes the computation and accurate reproduction of subtle shifts in reduction potentials for two mutants of the iron–sulfur protein *Pyrococcus furiosus* ferredoxin. The computational models involved only first-sphere ligands and differed with respect to one ligand, either acetate (aspartate), thiolate (cysteine), or methoxide (serine). Standard procedures using vacuum optimization gave qualitatively wrong results and errors up to 0.07 V. Using electrostatically screened geometries and large basis sets for expanding the wave functions gave quantitatively correct results, with errors of only 0.03 V. Correspondingly, only this approach predicted a change in the coordination mode of aspartate (i.e., a carboxylate shift) accompanying the reduction of the wild-type cluster, confirming results from synthetic models and explaining why electrostatic screening is necessary. Hence, the carboxylate shift appears to occur in the proteins from which data were collected. The results represent the most accurate predictions of shifts in reduction potentials for modified proteins, the success in part being due to the similar nature of the three amino acid ligands involved. The predicted carboxylate shift is expected to tune aspartate's degree of electron donation to the cluster's two oxidation states, thus making the reversible redox reaction feasible.

Introduction

This theoretical paper deals with the electronic structure of ligand-substituted 4Fe−4S clusters in *Pyrococcus furiosus* ferredoxin and aims toward reproducing and predicting shifts in reduction potentials and understanding their origin.

There are more than 160 iron−sulfur proteins known today, and although they are very similar in their chemical composition, they cover a wide range of functions, including electron transfer and catalysis as well as structural, regulatory, and sensory roles.[1,2] Because of their multifunctionality, small size, and early use in biological catalysis,[3] large potential is envisioned from understanding the design principles behind iron−sulfur clusters and applying this knowledge toward minimal-model rational design of new catalysts. iron−sulfur clusters modified in types of either metal ions or ligands can be ideally studied by computational approaches, where accuracy can be very high because of cancellation of common computational errors when comparing relative effects.

One very interesting example of modified clusters is found in a group of ferredoxins, which govern electron transfer in a large variety of organisms. The 4Fe−4S cluster of *P. furiosus* ferredoxin contains an aspartate instead of the typical cysteinate as one of its four amino acid ligands.[4] Site-directed mutagenesis has been applied to understand this puzzling modification of the wild-type protein; what are the advantages to using aspartate instead of cysteinate? Understanding such choices by nature can reveal important molecular information applicable to the analysis of other biological systems and may also help in modifying clusters for our own needs. Structures are not available for either wild-type or mutants, but accurate reduction potentials have been measured for the wild-type and two mutants,[4] providing a delicate test for computational modeling of these clusters. If passing such a test, modern computational chemistry may be anticipated to contribute a structure−function relationship for the observed properties, including a rationalization of the choice of aspartate made by nature in this particular case.

Computational studies of transition-metal systems have had a long history of calibration and development,[5−7] and density

* To whom correspondence should be addressed. E-mail: kpj@kemi.dtu.dk.

(1) Beinert, H.; Holm, R. H.; Münck, E. *Science* **1997**, *277*, 653−659.
(2) Johnson, M. K.; Smith, A. D. In *Encyclopedia of Inorganic Chemistry*, 2nd ed.; King, B. B., Ed.; Wiley: New York, 2005.
(3) Rees, D. C.; Howard, J. B. *Science* **2003**, *300*, 929−931.
(4) Brereton, P. S.; Verhagen, M. F. J. M.; Zhou, Z. H.; Adams, M. W. W. *Biochemistry* **1998**, *37*, 7351−7362.
(5) Siegbahn, P. E. M. *Adv. Chem. Phys.* **1996**, *93*, 333−387.

10.1021/ic7009836 CCC: $37.00
Published on Web 09/19/2007

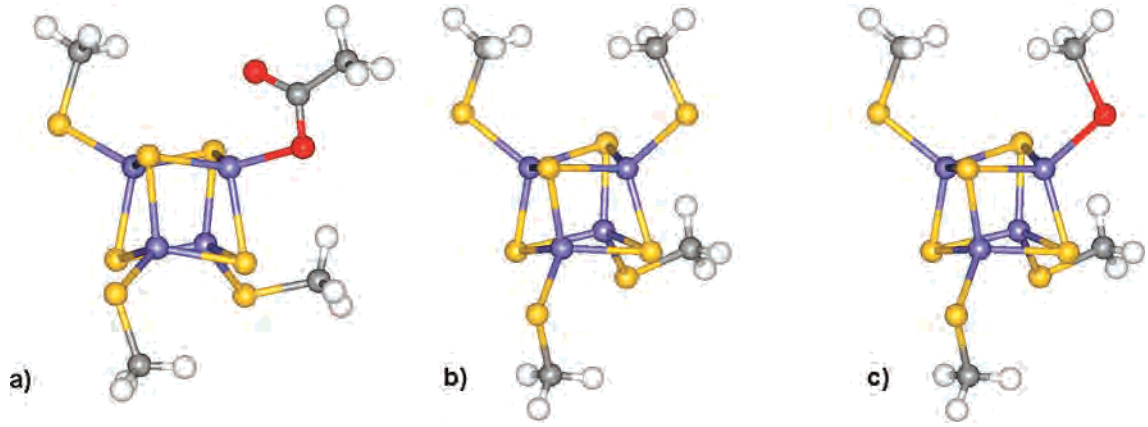

Figure 1. Structures of the models studied in this work: (a) wild-type cluster with aspartate (acetate); (b) D14C mutant with cysteine (methyl sulfide); (c) D14S mutant with serine (methoxide).

functional theory (DFT) is now considered the golden standard for obtaining geometries and energies of transition-metal-containing systems,[7,8] with typical errors smaller than 0.05 Å for metal−ligand bond lengths and 20 kJ/mol for reaction energies.[9] Iron−sulfur clusters constitute a difficult case in the sense that spin and close-lying configurations complicate the electronic structure. However, DFT should, in principle, be capable of reproducing all of the observed phenomena related to iron−sulfur clusters, assuming that a physically correct functional were to be applied, and many properties can be computed with DFT with high accuracy, including reduction potentials for 1Fe, 2Fe−2S, and 4Fe−4S clusters[10−12] and for full proteins[13] as well as reorganization energies,[14,15] transmission coefficients,[16] and NMR parameters.[17]

This work presents a detailed analysis of 4Fe−4S clusters with three different amino acid ligands, for which experimental reduction potentials are available in the case of *P. furiosus* ferredoxin.[4] The computational shifts are within 0.03 V of experimental shifts, which is unprecedented, with earlier computations giving relative reduction potentials within ca. 0.2 V for other, more different proteins.[10] The accuracy is mainly due to the fact that all three studied proteins are very similar, only differing in the nature of one amino acid ligand, which is in all cases negatively charged and of comparable size, and due to careful computation of comparable electronic structures. Importantly, the accurately computed shifts can be rationalized in terms of structure, with a change in the coordination mode of aspartate accompanying reduction of the wild-type cluster. Only a more physically correct electrostatic screening model accounts for this structural effect and thus for the experimentally observed shifts in reduction potentials, implying that the real protein is likely to undergo such a carboxylate shift upon reduction.

Theoretical Calculations

Model Systems. The computational models consisted of a complete cuboidal core, composed of four irons, four inorganic sulfides, and three thiolate ligands as models of cysteinates in the proteins, as shown in Figure 1. The fourth ligand was either acetate (as a model of wild-type aspartate), thiolate (as a model of cysteine), or methoxide (as a model of serine). The models are very electron-rich, with charges of −12 from the ligands, giving a total charge of −2 for the half-ferric, half-ferrous cluster. The clusters are referred to in the standard nomenclature, with the charges of the thiolates not included; i.e., the half-ferric, half-ferrous cluster is written as $[Fe_4S_4]^{2+}$. Models were based on a model of the all-cysteine $[Fe_4S_4]$ cluster, which was geometry-optimized and shown to be in good structural agreement with the experiment (see the Results and Discussion section).

Computational Details. Optimization of the cluster geometries was performed for all possible spin configurations and for the two relevant oxidation states, using the Becke-1988 exchange functional combined with the Perdew-1986 nonlocal correlation functional (BP86).[18,19] DFT energies involving substantial changes in orbital occupation suffer from the differential correlation effects encountered.[20,21] Thus, errors in ionization potentials are 30 kJ/mol even for diatomic transition-metal systems.[22] In particular, the treatment of interactions between electrons of the same spin (Fermi correlation) differs between functionals. Specific problems include spin-splitting energies[8] and bond dissociation energies,[23] with hybrid functionals such as B3LYP well-known to favor the open-shell, spin-polarized cases more than generalized gradient approximation (GGA) functionals such as BP86.[23] It has been seen that several GGA and hybrid functionals reproduce the correct spin state of small transition-metal systems, with no clearly superior functional

(6) Ziegler, T. *Chem. Rev.* **1991**, *91*, 651−667.
(7) Frenking, G.; Frohlich, N. *Chem. Rev.* **2000**, *100*, 717−774.
(8) Siegbahn, P. E. M. *J. Biol. Inorg. Chem.* **2006**, *11*, 695−701.
(9) Siegbahn, P. E. M.; Blomberg, M. R. A. *Chem. Rev.* **2000**, *100*, 421−437.
(10) Torres, R. A.; Lovell, T.; Noodleman, L.; Case, D. A. *J. Am. Chem. Soc.* **2003**, *125*, 1923−1936.
(11) Kennepohl, P.; Solomon, E. I. *Inorg. Chem.* **2003**, *42*, 689−695.
(12) Mouesca, J.-M.; Chen, J. L.; Noodleman, L.; Bashford, D.; Case, D. A. *J. Am. Chem. Soc.* **1994**, *116*, 11898−11914.
(13) Stephens, P. J.; Jollie, D. R.; Warshel, A. *Chem. Rev.* **1996**, *96*, 2491−2513.
(14) Sigfridsson, E.; Olsson, M. H. M.; Ryde, U. *Inorg. Chem.* **2001**, *40*, 2509−2519.
(15) Sigfridsson, E.; Olsson, M. H. M.; Ryde, U. *J. Phys. Chem. B* **2001**, *105*, 5546−5552.
(16) Kennepohl, P.; Solomon, E. I. *Inorg. Chem.* **2003**, *42*, 696−708.
(17) Machonkin, T. E.; Westler, W. M.; Markley, J. L. *Inorg. Chem.* **2005**, *44*, 779−797.
(18) Becke, A. D. *Phys. Rev. A* **1988**, *38*, 3098−3100.
(19) Perdew, J. P. *Phys. Rev. B* **1986**, *33*, 8822−8824.
(20) Harrison, J. F. *Chem. Rev.* **2000**, *100*, 679−716.
(21) Neese, F. *J. Biol. Inorg. Chem.* **2006**, *11*, 702−711.
(22) Jensen, K. P.; Roos, B. O.; Ryde, U. *J. Chem. Phys.* **2007**, *126*, 014103.
(23) Jensen, K. P.; Ryde, U. *J. Phys. Chem. A* **2003**, *107*, 7539−7545.

available.[22] For some properties, functionals other than B3LYP perform better,[22,24,25] and BP86 geometries of transition-metal diatomics are in slightly better agreement with experiment.[22] For the problem at hand, only closed-shell perturbations occur upon changing of the ligands, and B3LYP is thus expected to show a comparable performance.

The basis set used for geometry optimization was 6-31G(d) for all atoms, whereas metal ions were assigned a TZVP basis set. This basis set is referred to as medium-sized (M).[26] Accurate energies were subsequently calculated on the equilibrium structures with the 6-311+G(2d,2p) and def2-TZVPP basis sets, which include additional functions with small exponents, to take into account the tail of the diffuse electron density encountered in the negatively charged clusters.

The computations were carried out with the *Turbomole* program,[27] version 5.8. All geometry optimizations were carried out in redundant internal coordinates using the Cosmo model (vide infra) or the standard procedure. Fully unrestricted calculations were performed for all Kohn−Sham configurations. Electronic structures were considered self-consistent when electronic energies were converged down to 10^{-6} Hartree (2.6 J/mol) and the largest gradient norm was converged down to 10^{-3} au. Zero-point energies were calculated on vacuum geometries because Cosmo is not implemented with frequency analysis. All ground-state species were true minima on the potential energy surfaces, without any imaginary frequencies. Atomic charges and spin densities were calculated from Mulliken population analysis using the def2-TZVPP basis set. Absolute, but not relative, values are quite basis-set-dependent and thus not very informative.

To succeed in the ambitious goal of reproducing subtle shifts in reduction potentials between very similar clusters, it is paramount that the same ground-state electronic structure is obtained for all clusters, to render any comparison meaningful. To help in this procedure, geometry optimizations were initiated from common coordinates and electronic configurations were converged for large M_S quantum numbers, to allow for an accurate and similar spin coupling in all three clusters. Subsequently, convergence of the low-spin symmetry-broken configurations was obtained using the converged orbitals of the high-spin configurations as input, and starting from orbital sets of all M_S values up to 7 or 8, to make sure the lowest energy is obtained for all three clusters, in accordance with the (Hohenberg−Kohn) variational principle. If such a procedure is not followed, the obtained low-spin configurations are likely to be local minima and comparison would not be meaningful for the present scope.

The Cosmo Model. It turned out that the standard procedure of optimizing geometries in vacuum with a M basis set did not provide geometries of the expected accuracy when comparing with experiment. In order to correct for this discrepancy, we performed all geometry optimizations with the conductor-like screening model (Cosmo)[28,29] taken into account iteratively, as is possible in *Turbomole*. In this method, the solute molecule forms a cavity within a dielectric continuum characterized by a dielectric constant, ϵ. The charge distribution of the solute polarizes the dielectric medium, and the response of the medium is described by the generation of screening charges on the surface of the cavity. These computations were performed with dielectric constants of 4 and 80, sufficient to screen the charges in the cluster and resembling a more physically correct situation, as evidenced by the better agreement with experimental cluster and protein structures (see the Results and Discussion section). Furthermore, the screening turned out to be critical for modeling the change in the coordination mode of the aspartate ligand of the wild-type cluster. For the generation of the cavity, a set of atomic radii has to be defined. The optimized Cosmo radii in *Turbomole* were applied (H, 1.30 Å; C, 2.00 Å; S, 2.16 Å).[30] The radii for all metals were set to 2.0 Å and are insensitive to the energies because of their buried nature. Shifts in reduction potentials between two clusters A and B were derived from the large (L) basis set energies with the Cosmo screening using $\epsilon = 80$, according to eq 1. Here, $\Delta E_{AB}^{Cosmo}(ox)$ refers to the

$$\Delta E_{AB}^{0} = \Delta E_{AB}^{Cosmo}(ox) - \Delta E_{AB}^{Cosmo}(red) \quad (1)$$

difference in Cosmo energies of the oxidized forms of clusters A and B. The shifts in reduction potentials accompanying the change of the environment in the clusters should be accurately described to substantially less than the earlier 0.2 V[10] because the environment is, in fact, the same (absent) protein in our case and because errors in relative potentials will tend to cancel for mutants with electronically similar modified amino acids, provided that the correct and similar electronic structures are indeed computed for the clusters.

Table 1. Computed Energies (kJ/mol) of Electronic Configurations for the Biologically Relevant Oxidation States of the Three $[Fe_4S_4]Cys_3X$ Clusters (X = Asp, Cys, Ser)[a]

	$[Fe_4S_4]^{+}$				$[Fe_4S_4]^{2+}$		
M_S	Asp	Cys	Ser	M_S	Asp	Cys	Ser
1	0	0	0	0	0	0	0
3	43	40	55	2	45	49	48
5	43	53	62	4	67	70	77

[a] M_S signifies an excess number of spin-up electrons in the electronic configuration, using basis set M.

Results and Discussion

The spins observed experimentally are low-spin for all three clusters,[31] because of antiferromagnetic coupling of each of the four high-spin iron centers. This situation is also obtained from our computations, as shown in Table 1. In both oxidation states of all three clusters, the electronic configuration having the minimum number of excess spin-up electrons is the lowest in energy, favored by 40−55 kJ/mol to the intermediate-spin configuration, which is a comfortable margin. Thus, the present methodology is capable of obtaining an electronic structure consistent with the experimentally observed antiferromagnetic coupling, and this gives some confidence in the nature of the computed electronic structures. In addition, the similar closeness of the higher spin configurations confirms that the same general electronic structure was obtained in all three cases.

(24) Zhao, Y.; Schultz, N. E.; Truhlar, D. G. *J. Chem. Phys.* **2005**, *123*, 161103.
(25) Schultz, N. E.; Zhao, Y.; Truhlar, D. G. *J. Phys. Chem. A* **2005**, *109*, 11127−11143.
(26) Schäfer, A.; Horn, H.; Ahlrichs, R. *J. Chem. Phys.* **1992**, *97*, 2571−2577.
(27) Alrichs, R.; Bär, M.; Häser, M.; Horn, H.; Kölmel, C. *Chem. Phys. Lett.* **1989**, *162*, 165−169.
(28) Klamt, A.; Schüürmann, J. *J. Chem. Soc., Perkin Trans.* **1993**, *2*, 799−805.
(29) Schäfer, A.; Klamt, A.; Sattel, D.; Lohrenz, J. C. W.; Eckert, F. *Phys. Chem. Chem. Phys.* **2000**, *2*, 2187−2193.
(30) Klamt, A.; Jonas, V.; Bürger, T.; Lohrenz, J. C. W. *J. Phys. Chem. A* **1998**, *102*, 5074−5085.
(31) Calzolai, L.; Zhou, Z. H.; Adams, M. W. W.; La Mar, G. N. *J. Am. Chem. Soc.* **1996**, *118*, 2513−2514.

Table 2. Calculated and Experimental Fe−S Bond Lengths and Mean Absolute Errors (MAEs) for the $[Fe_4S_4]^{2+}$ Clusters Compared with Experiment[a]

	average $Fe-S_{thiolate}$ bonds	average long $Fe-\mu_3$-S bonds	average short $Fe-\mu_3$-S bonds
calcd (80)	2.25	2.32	2.22
calcd (4)	2.26	2.32	2.22
calcd (1)	2.28	2.33	2.23
expt[b]	2.25	2.31	2.24
MAE (80)	0.00	0.01	0.02
MAE (4)	0.01	0.01	0.02
MAE (1)	0.03	0.02	0.01

[a] Cosmo with $\epsilon = 4$ and 80 and vacuum (1) geometry optimization procedures. [b] The analogue in the $[Fe_4S_4]^{2+}$ oxidation state, with four SCH_2Ph ligands.[37]

Table 2 shows the Fe−S bond lengths obtained for the $[Fe_4S_4]^{2+}$ all-thiolate cluster, for which analogues with high-resolution X-ray structures are available. Experimental data indicate that, in both proteins and synthetic analogues, four $Fe-\mu_3$-S bonds are somewhat (typically ca. 0.05 Å) shorter than the other eight $Fe-\mu_3$-S bonds.[32] Thus, in Table 2, these two groups of long and short $Fe-\mu_3$-S bonds have been distinguished. Importantly, the computations also exhibit this pattern.

Overall, the computed structures are in very good agreement with the structure of the synthetic analogue. In fact, agreement is even better than could be expected from mean absolute errors of ca. 0.03 Å for metal−ligand bond lengths in transition-metal diatomics.[22] We obtain mean absolute errors in bond lengths of only 0.01 Å for the Cosmo models and 0.02 Å for the vacuum models. The largest effect is seen in the $Fe-S_{thiolate}$ bonds, where the Cosmo optimization shortens bonds 0.02−0.03 Å down to the experimental values. The Cosmo-optimized structures are in better agreement with the experimental structure for both $\epsilon = 4$, which is a lower bound to the value expected in a protein, and $\epsilon = 80$, resembling water. This is due to better dispersion of the excess electronic charge of the cluster. The two choices of dielectric constants give similar bond lengths within 0.01 Å, and a value of 80 was subsequently used for geometry optimizing all structures.

Having established that the BP86-Cosmo-optimized models provide electronic structures in excellent agreement with experiment, we now turn to the more difficult task of computing the shift in reduction potentials accompanying site-directed mutagenesis of the clusters in the protein *P. furiosus* ferredoxin.[4,32] Computations of reduction potentials for 4Fe−4S[10,12] and 3Fe−4S clusters[13] have been performed earlier with DFT methods, with typical errors in shifts of 0.2 V. Here, the focus is on the subtle shifts in reduction potentials caused by substitution of electronically similar ligands. These shifts are quite small, on the order of 50−100 mV, or ca. 5−10 kJ/mol. Normally, state-of-the-art computational chemistry cannot reproduce such energy differences, but because of the largely electrostatic nature of the perturbations and the essentially intact electronic structures of the mutants, we will show that these shifts can, in fact, be computed with very high accuracy.

Protein reduction potentials are quite different from cluster reduction potentials.[32] Thus, the experimentally observed role of the protein in tuning E^0 by more than half a volt is in agreement with the magnitude estimated theoretically.[13] However, relative reduction potentials can be computed assuming that first-sphere models provide the majority of the effect, knowing that the remaining protein is of identical composition in the present case. With such an approach, computed energies become so accurate that it can be concluded that the surrounding changes in the protein structure do not affect the magnitude of the shift in reduction potentials caused by mutation.

Let us first look at geometry-optimized clusters using Cosmo, with energies computed with the M basis set. This basis set does not include diffuse functions and is thus expected to encounter problems when computing the change in the diffuse electron density accompanying reduction of the already electron-rich clusters. However, because the electronic structures of wild-type and mutants are quite similar, the tails of the electron densities are also expected to be similar in corresponding oxidation states of the wild-type and mutants, and one may expect decent results for a computed shift in reduction potentials. The results are shown in Table 3, where computational shifts are compared to the temperature-independent data at 23 °C, because temperature-dependent data (in parentheses) were fitted up to 100 °C. These shifts differ by less than 0.02 V. The computed shifts are qualitatively correct. However, the Asp−Cys shift is not very accurate, being 0.06 V experimentally,[4] but is found to be only 0.01 V from computation. Although these energy differences are quite small in energy units and satisfactory for most computational purposes, the accuracy can be expected to improve if the size of the basis set is increased.

Table 4 shows the corresponding results when the larger 6-311+G(2d,2p) basis set including diffuse functions is used on the Cosmo-optimized structures. The shifts are now correctly reproduced both qualitatively and quantitatively, with errors of 0.02 V or less. This is an unusually accurate result, which indicates that, for simple mutations involving similar amino acids (all negatively charged), the electrostatic closed-shell perturbation of the electronic structure can be modeled to an astonishing accuracy of ca. 2 kJ/mol. Larger errors can be expected when amino acids differ more; e.g., in terms of charge, if spin changes during mutation or if the exact corresponding electronic configurations are not obtained during the computational procedure. Table 5 shows the corresponding results with the large def2-TZVPP basis set, which has diffuse functions and up to *g* functions in the contraction for iron. This basis set gives similar results, however with the Ser−Asp shift computed to be 0.03 V to large, still in very good agreement with experiment.

We now look at the corresponding results for the L basis set, using the geometries obtained from a standard optimization procedure without electrostatic screening. The results, shown in Table 6, indicate large errors and not even a qualitatively correct prediction of the shifts in reduction

(32) Venkateswara, P.; Holm, R. H. *Chem. Rev.* **2004**, *104*, 527−559.

Table 3. Computed and Experimental Reduction Potentials (V) Using the M Basis Set and Cosmo-Optimized Geometries

ligand in protein	E^0(exp)[a]	ligand in model[b]	E^0(calc)	Asp = 0		ΔE^0(exp) − ΔE^0(calc)
				ΔE^0(exp)[c]	ΔE^0(calc)	
Asp	−0.368	CH_3COO^-	−1.73	0	0	
Cys	−0.426	CH_3S^-	−1.74	0.06 (0.04)	0.01	0.05
Ser	−0.501	CH_3O^-	−1.86	0.13 (0.12)	0.13	0.00

[a] Reference 4. [b] See Figure 1. [c] Data in parentheses are experimental temperature-dependent data.

Table 4. Computed and Experimental Reduction Potentials (V) Using the 6-311+G(2d,2p) Basis Set and Cosmo-Optimized Geometries

ligand in protein	E^0(exp)[a]	ligand in model[b]	E^0(calc)	Asp = 0		ΔE^0(exp) − ΔE^0(calc)
				ΔE^0(exp)[c]	ΔE^0(calc)	
Asp	−0.368	CH_3COO^-	−1.38	0	0	
Cys	−0.426	CH_3S^-	−1.44	0.06 (0.04)	0.06	0.00
Ser	−0.501	CH_3O^-	−1.50	0.13 (0.12)	0.12	0.01

[a] Reference 4. [b] See Figure 1. [c] Data in parentheses are experimental temperature-dependent data.

Table 5. Computed and Experimental Reduction Potentials (V) Using the def2-TZVPP Basis Set and Cosmo-Optimized Geometries

ligand in protein	E^0(exp)[a]	ligand in model[b]	E^0(calc)	Asp = 0		ΔE^0(exp) − ΔE^0(calc)
				ΔE^0(exp)[c]	ΔE^0(calc)	
Asp	−0.368	CH_3COO^-	−1.36	0	0	
Cys	−0.426	CH_3S^-	−1.43	0.06 (0.04)	0.07	−0.01
Ser	−0.501	CH_3O^-	−1.52	0.13 (0.12)	0.16	−0.03

[a] Reference 4. [b] See Figure 1. [c] Data in parentheses are experimental temperature-dependent data.

Table 6. Computed and Experimental Reduction Potentials (V) Using the L Basis Set and Vacuum-Optimized Geometries

ligand in protein	E^0(exp)[a]	ligand in model[b]	E^0(calc)	Asp = 0		ΔE^0(exp) − ΔE^0(calc)
				ΔE^0(exp)[c]	ΔE^0(calc)	
Asp	−0.368	CH_3COO^-	−1.50	0	0	
Cys	−0.426	CH_3S^-	−1.49	0.06 (0.04)	−0.01	0.07
Ser	−0.501	CH_3O^-	−1.69	0.13 (0.12)	0.19	−0.06

[a] Reference 4. [b] See Figure 1. [c] Data in parentheses are experimental temperature-dependent data.

Table 7. Computed and Experimental Reduction Potentials (V) Using the L Basis Set and Cosmo-Optimized Geometries, Including Zero-Point Corrections

ligand in protein	E^0(exp)[a]	ligand in model[b]	E^0(calc)	Asp = 0		ΔE^0(exp) − ΔE^0(calc)
				ΔE^0(exp)[c]	ΔE^0(calc)	
Asp	−0.368	CH_3COO^-	−1.32	0	0	
Cys	−0.426	CH_3S^-	−1.38	0.06 (0.04)	0.06	0.00
Ser	−0.501	CH_3O^-	−1.42	0.13 (0.12)	0.10	0.03

[a] Reference 4. [b] See Figure 1. [c] Data in parentheses are experimental temperature-dependent data.

potentials, with the wrong direction predicted for the Asp−Cys shift (−0.01 V vs experimental +0.06 V). Thus, it can be concluded that electrostatic screening of the geometry is essential for obtaining accurate shifts in reduction potentials and standard geometry optimizations will not suffice to reproduce the subtle effects involved here.

Furthermore, we have computed the effect of zero-point energies on the shifts in reduction potentials. The zero-point energies were calculated from vibrational analysis at the BP86/6-31G(d) level, which confirmed that all ground states are stationary minima on the potential energy surface (no imaginary frequencies). Table 7 shows the L basis set energies from Cosmo as in Table 4 but including the zero-point energies. Agreement is similar to Tables 4 and 5 (0.03 V) for the larger Asp−Ser shift. However, Table 7 confirms the accuracy of the approach and shows that zero-point effects essentially cancel in the evaluation of the shifts.

The screening was chosen to be a waterlike environment, whereas the screening in the proteins is heterogeneous. However, it can be concluded that the exact value of the screening is less important, as long as it substantially dampens the electrostatic repulsion in the models, in particular affecting the Fe−O and Fe−$S_{thiolate}$ bonds. The fact that the geometrical effect is larger than the basis set effect points toward the importance of the changes in the Fe−O and Fe−$S_{thiolate}$ bond lengths upon reduction. We shall briefly discuss these structural changes to explain the subtle shifts in more detail.

Table 8 shows the optimized bond lengths for Fe−X bonds, where X is the coordinating atom of the mutated residue. It is seen that the Fe−X bonds are shorter in the Cosmo-optimized structures because of the reduced electrostatic repulsion in the clusters. Furthermore, the oxidized structures have shorter Fe−X bonds by ca. 0.03 Å with the Cosmo model and 0.04−0.06 Å for the vacuum structures. Aspartate is an exception because it binds in a preferably monodentate fashion in most structures. However, the second oxygen is much closer to iron in the Cosmo-optimized

Table 8. Bond Lengths for Fe−X Bonds (Å), Where X Is the Coordinating Atom of the Mutated Residue, Geometry-Optimized with Cosmo (C) or Vacuum (V) Procedures

	Fe−X (C)		Fe−X (V)	
ligand in protein	$[Fe_4S_4]^{2+}$	$[Fe_4S_4]^{+}$	$[Fe_4S_4]^{2+}$	$[Fe_4S_4]^{+}$
Asp[a]	2.03/2.45	1.97/3.05	1.94/3.31	2.00/3.65
Cys	2.25	2.28	2.28	2.32
Ser	1.84	1.87	1.86	1.91

[a] For Asp, both oxygen distances to Fe are included.

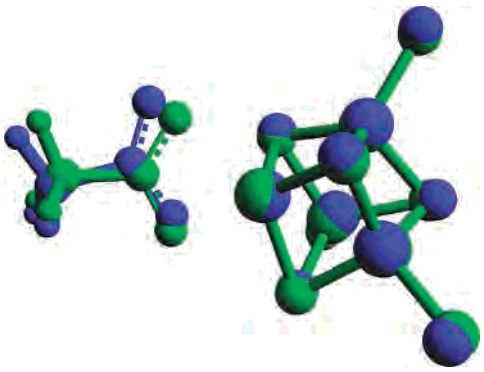

Figure 2. Computed carboxylate shift accompanying the reduction of the wild-type cluster. Green: oxidized. Blue: reduced. The model of aspartate is shown to the left, with the 4Fe−4S cluster to the right.

geometries. This is particularly true for the oxidized $[Fe_4S_4]^{2+}$ state, which is essentially bidentate, and this leads to elongation of the tighter bound oxygen from 1.97 to 2.03 Å, so that this oxygen is actually closer to iron in the reduced structure. Thus, aspartate undergoes a carboxylate shift upon reduction, according to the computations. The electrostatic screening accounts for this interesting difference between the Cosmo and vacuum models and can explain why the vacuum model does not predict the shifts in reduction potentials correctly. The computed monodentate distances are in good accord with iron−carboxylate distances of 1.95−2.08 Å found in some diiron complexes.[33]

For comparison, carboxylate shifts in diiron model complexes correspond to monodentate Fe−O bonds of 2.01/3.06 Å and bidentate bonds of 2.02−2.06/2.32−2.49 Å,[34] in excellent agreement with our results of 1.97/3.01 and 2.03/2.45 Å. A well-known case in which a carboxylate shift to iron has been observed is ribonucleotide reductase, which is a redox-active enzyme and may benefit from the same tuning of electron donation available from such a shift.[35]

The change in the coordination mode for the geometry-optimized structures of the reduced (blue) and oxidized (green) wild-type clusters is shown in Figure 2. The bidentate structure observed for the oxidized cluster of the wild-type protein when using the Cosmo model is in agreement with conclusions drawn from spectroscopic analysis of similar synthetic models.[36] It has not been possible for us to study whether it is also true as suggested[31] that this structural change "gates" the electron transfer. However, the carboxylate shift is necessary to reproduce experimental data and thus appears to be occurring in the wild-type protein. The carboxylate shift observed in our computations must be an important reason why aspartate is found in wild-type *P. furiosus* ferredoxin. A shifting aspartate allows for more electron donation to the oxidized state and less to the reduced state and thus renders both reduction and oxidation of the cluster more feasible.

Table 9. Changes in the Atomic Charges upon Reduction in the Three Clusters[a]

					S^{2-}			
ligand	Fe1	Fe2	Fe3	Fe4[b]	1	2	3	4
Asp[a]	−0.07	−0.06	−0.10	+0.08	0.17	0.15	0.17	0.16
Cys	−0.08	−0.05	−0.10	+0.02	0.18	0.15	0.19	0.15
Ser	−0.05	−0.04	−0.06	−0.01	0.18	0.16	0.16	0.16

[a] Positive indicates more electron density upon reduction. [b] Binds to the mutated ligand.

As seen in Table 9, the reducing electron is delocalized over the entire cluster in the DFT description, with the sulfides taking up the majority of the excess electron density. All clusters exhibit the same amount of electron delocalization (ca. 0.65 e) onto the sulfides, indicating similar electronic structures of reduced and oxidized states, respectively, in all clusters. The remaining electron density goes into the sulfur atoms of the thiolates, with essentially no electron density ending up on mutated groups or on the methyl groups of the thiolates. Three of the irons lose a little electron density upon reduction, perhaps an effect of the Mulliken partition scheme when geometries change or indicating a larger polarization, with ionic Fe^{+}/S^{-} configurations contributing to the reduced wave function. However, the most significant change, although still subtle, is the 0.08 increase electron density on Fe4 bound to the mutated ligand, in the aspartate wild-type. Altogether, the charge changes are very minor and comparable in all clusters, indicating their similar electronic structures.

The qualitative nature of the antiferromagnetic coupling can be confirmed from Figure 3, which shows the atomic spin densities on iron atoms in reduced and oxidized states of the three clusters. These spins are accompanied by approximately half a spin up and half a spin down on the sulfur atoms. The oxidized all-cysteine cluster displays an electronic structure with four equivalent $Fe^{2.5}$ sites, with ca. 3.0 unpaired electrons assigned to iron atomic orbitals plus 0.5 from sulfur atomic orbitals, two being spin up and two being spin down. The reduced cluster has additional spin-up density, which is spin-polarized two give two equivalent Fe_2 sites. In the aspartate and serine clusters, this symmetry is broken, and interestingly, the iron atom binding to the oxygen exhibits more spin density in both reduced and oxidized states. However, the general qualitative picture of antiferromagnetic coupling remains valid in all clusters.

The shifts in reduction potentials can be reproduced from models that only include first-sphere ligands with β-carbons

(33) Nielsen, M. S.; Harris, P.; Ooi, B.-L.; Christensen, H. E. M. *Biochemistry* **2004**, *43*, 5188−5194.
(34) Kuzelka, J.; Spingler, B.; Lippard, S. J. *Inorg. Chim. Acta* **2002**, *337*, 212−222.
(35) LeCloux, D. D.; Barrios, A. M.; Mizoguchi, T. J.; Lippard, S. J. *J. Am. Chem. Soc.* **1998**, *120*, 9001−9014.
(36) Andersson, M. E.; Hogbom, M.; Rinaldo-Matthis, A.; Andersson, K. K.; Sjoberg, B. M.; Nordlund, P. *J. Am. Chem. Soc.* **1999**, *121*, 2346−2352.

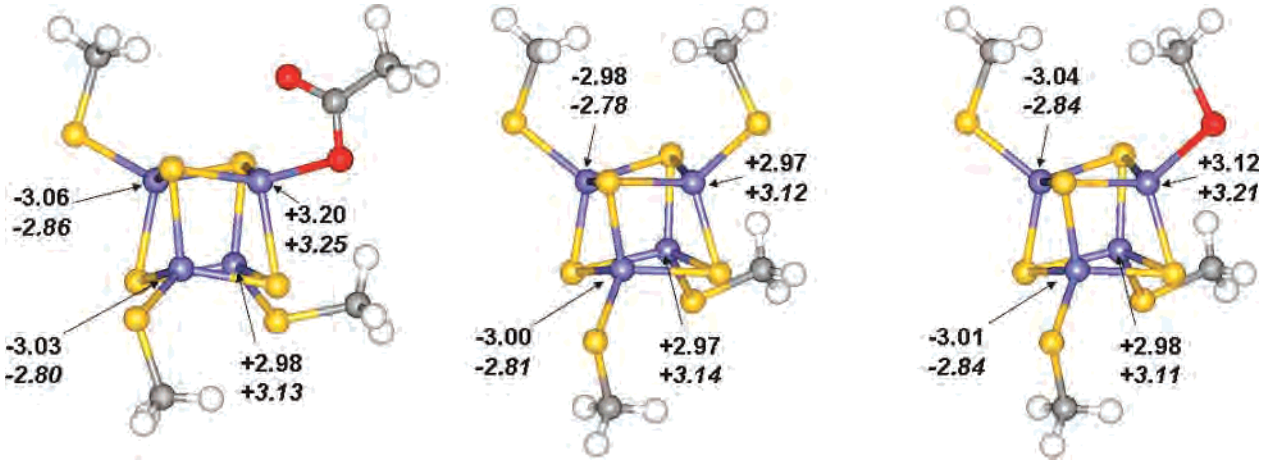

Figure 3. Atomic spin densities of iron in oxidized (top) and reduced (bottom, italics) aspartate (left), cysteine (middle), and serine (right) clusters.

of amino acids, provided electrostatic screening is correctly accounted for. This shows directly that changes in the protein structure beyond this do not contribute to the shifts in the potentials of more than 10 mV in this case. The reason is likely to be the similarity in the size and charge of the amino acids of the mutants to that of the wild-type, causing minor distortion of the remaining protein. The impressive results obtained for mutants of iron−sulfur proteins from a molecular-dynamics-relaxed protein−dipole Langevin−dipole model[13] had deviations between 28 and 119 mV, using a purely classical model but accounting for the entire proteins. The energy components included to compute these shifts all involved interactions between the iron−sulfur cluster and the surroundings, of which the first sphere can be expected to dominate. Hence, both works indicate that other interactions involving only protein and solvent are not important to model the shifts in reduction potentials.[13] DFT computations on less similar clusters gave typical errors in shifts of 0.20 V.[10] That we can reach an accuracy of 0.03 V for some types of mutations is an encouraging result that can hopefully be used to study redox properties of simply modified proteins in the future.

In conclusion, a structure−function relationship has been suggested from the present computations in the absence of experimental structures of any of the oxidation states or mutants. Standard DFT calculations exhibit qualitative errors in computed shifts in reduction potentials between cluster types and at the same time do not reveal a carboxylate shift upon reduction of the wild-type cluster. On the other hand, the electrostatic screening model yields excellent shifts in reduction potentials between clusters *and* predicts a corresponding carboxylate shift upon reduction of the wild-type cluster, in accordance with the bidentate binding mode of carboxylate in the $[Fe_4S_4]^{2+}$ state in model complexes.[37] Hence, there is strong reason to conclude that the structural change described in Figure 2 indeed takes place when wild-type *P. furiosus* ferredoxin is reduced. Such a structural change allows for a modification of the electronic charge available to the cluster, with more electron density in the bidentate form stabilizing the higher oxidation state. This situation renders both reduction and oxidation easier, facilitating reversibility of the redox reaction.

Acknowledgment. This work was made possible by the Velux Foundation through a Villum−Kann−Rasmussen fellowship and by The Danish Natural Science Research Council (Grant 21-04-0392). Computer time provided by the Danish Center for Scientific Computing and the Center for Sustainable and Green Chemistry at the Technical University of Denmark is gratefully acknowledged.

IC7009836

(37) Weigel, J. A.; Holm, R. H. *J. Am. Chem. Soc.* **1991**, *113*, 4184−4191.